

Eddy current effects in a high field dipole

Man-Zhou Zhang¹ · Miao Zhang¹ · Xiu-Cui Xie¹ · Song-Qing Tan¹ ·
Ji-Dong Zhang¹ · Lian-Hua Ouyang¹ · Rui Li¹ · De-Ming Li¹

Received: 17 March 2017 / Revised: 6 June 2017 / Accepted: 8 August 2017 / Published online: 16 November 2017

© Shanghai Institute of Applied Physics, Chinese Academy of Sciences, Chinese Nuclear Society, Science Press China and Springer Nature Singapore Pte Ltd. 2017

Abstract Eddy currents produced by a time-varying magnetic field will introduce time delay and thus affect field quality. This effect leads to drifting of the beam position over time, especially for a compact synchrotron. Simulations and measurements of different dipoles have been performed, to investigate the time delay and field quality. The simulations are conducted using OPERA software. The measurements are conducted using a long coil and Hall sensor. All results show that the magnetic field deviation is up to 0.4% for the dipole with stainless steel endplates. The simulations show that the main sources of eddy current are the field saturation effect and the field component B_z , introduced by the bedstead-type coil. Field correction using a power supply is adopted to reduce the deviation to less than 0.02%.

Keywords Eddy current · Time delay · Magnetic field measurement · Dipole · Field control

1 Introduction

The proton is one of the best particles for use in tumor treatment as the Bragg peaks that indicate the most energy lost occur at the end of its particle trace. The position of the Bragg peaks is determined by the proton energy. The typical

energy required for cancer therapy is 70–250 MeV [1, 2]. As the energy can be changed more easily for a synchrotron than that for a cyclotron [3], synchrotrons are employed as the main accelerator in several facilities. The treatment requires a long, stable extraction spill that can be obtained by the third-order slow resonant extraction [4–7]. For slow extraction, a large horizontal beam stay clear of more than 130 mm should be sustained [8]. Therefore, the apertures of all magnet elements are very large. On the other hand, in order to reduce the size of accelerator, the magnetic field of the main dipole should be very high. The main design parameters of a dipole are listed in Table 1. The static local and integrated field quality was designed carefully and optimized by using the tools named Poisson and OPERA. A prototype was manufactured. The measurement results show that the static field quality satisfied the requirements.

A Rogowski profile [9, 10] and laminated yoke are adopted to reduce eddy current, though in the rapidly changing magnetic field, the eddy current effect is not negligible. Eddy current introduces a time delay and affects field quality [11]. The time-varying eddy current causes drifting of the beam position over time [12]. Globally, attempts have been made to reduce the eddy current effect via simulations, optimizations, measurements, and compensation using a power supply [9–17]. In this paper, the simulations, measurements, and compensation of a high field dipole are described.

2 Eddy current in a dipole and its effect on the beam

The eddy current in magnets has been studied in detail since the 1970s. Reference [11] gives a detailed description of eddy currents. According to Faraday's law, a time-

This work was supported by the Youth Innovation Promotion Association of Chinese Academy of Sciences (No. 20150210).

✉ Miao Zhang
zhangmiao@sinap.ac.cn

¹ Shanghai Institute of Applied Physics, Chinese Academy of Sciences, Shanghai 201800, China

Table 1 Design parameters of a high field dipole

Type of the magnets	H-type
Magnetic effective length (m)	1.1
Bending angle (°)	45
Magnetic field at injection (T)	0.274
Min. magnetic field at extraction (T)	0.879
Max. magnetic field at extraction (T)	1.737
Max. magnetic field ramp rate (T/s)	2
Type of the coils	Bedstead

varying magnetic flux induces a voltage in a conductor loop; this voltage drives the eddy current flowing in the loop. Subsequently, the eddy current creates an additional magnetic field. The additional magnetic field is in the direction opposite to the change in magnetic flux, and the final magnetic field resulting from the initial and additional magnet field lags behind. When the changes in magnetic flux cease, the eddy current does not disappear immediately. This effect is the so-called time delay. Higher magnetic field and larger magnetic ramp rate lead to considerably larger amplitudes and longer delays. The time constant of the time delay depends on lamination thickness, materials (conductivity σ and iron permeability μ), packing factor, magnetic field strength, and magnetic flux change rate [11]:

$$\tau_n = \frac{d^2}{n^2 \pi^2 \kappa}, \tag{1}$$

where $\kappa = \frac{d}{\sigma \mu}$ for a slab and $\kappa = \frac{g}{\sigma \mu_0 l}$ for a C-type dipole; μ_0 is the permeability in air; g is the gap; l is the magnet length; d is the lamination thickness; and n is the order. The time constant is the sum over different n . A real magnet has limited length and thus a longitudinal magnetic field component. The iron permeability changes with the position and with the magnetic field.

The time delay of dipoles in a synchrotron leads to a mismatch between the magnetic field and frequency of the radio frequency system. The mismatch leads to beam momentum errors and forces the beam to circulate in a dispersive orbit. The mismatch gradually disappears because the eddy current decreases with time. The beam then attains a stable position. The distance from the stable orbit to the dispersive orbit is

$$\Delta x = D \frac{\Delta p}{p}, \tag{2}$$

where D is the dispersion function.

The relationship of the revolution frequency difference Δf , momentum difference Δp , and magnetic field deviation ΔB can be written as follows:

$$\frac{\Delta f}{f} = \left(\frac{1}{\gamma_t^2} - \frac{1}{\gamma^2} \right) \frac{\Delta p}{p} + \frac{1}{\gamma_t^2} \frac{\Delta B}{B}, \tag{3}$$

where γ is the relativity factor and γ_t is the transition energy of a synchrotron.

If the beam energy greatly exceeds the transition energy, the momentum difference in the synchronous particle is

$$\frac{\Delta p}{p} \approx \frac{\Delta B}{B}. \tag{4}$$

However, the energy of extraction protons is very close to the transition gamma of a compact synchrotron [2]. For 250-MeV protons, the momentum difference in the synchronous particle is as follows:

$$\frac{\Delta p}{p} \approx 2 \frac{\Delta B}{B}. \tag{5}$$

If the maximum dispersion is 2.3 m, a magnetic field deviation of 0.2% will cause a dispersion orbit of up to 9.2 mm. This large orbit not only moves the beam, but also leads to beam loss. Because the time delay considerably affects the beam, time-dependent magnetic fields have gained great attention.

3 AC magnetic field measurement

Two prototypes with endplates of different materials—stainless steel (named ST dipole) and pure iron (named DT4 dipole)—are fabricated for the magnetic field test. An AC magnetic field measurement system is set up, as shown in Fig. 1. A long coil is used for integral magnetic field measurement at the central line. The voltage induced by varying the magnetic field is measured and integrated. A Hall sensor is used for measuring the magnetic field at different points. The current of the power supply is measured by a high-precision direct current transform (DCCT) at the same time. Two digital data acquisition (ADC) cards simultaneously collect the signals from long coil and Hall sensor, and the DCCT. The actual resolution of the ADC is 0.67 ppm at 1 kHz. The long-term stability is less than 5 ppm in 24 h.

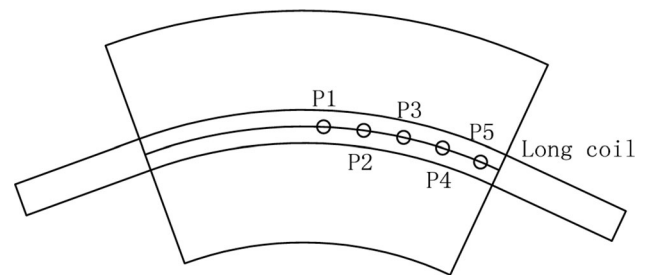


Fig. 1 Positions of the long coil and Hall sensor

The magnetic field at different ramp rates and maximum currents of the power supply are measured to understand the eddy current. Figure 2 shows the normalized current, integral magnetic field, and the magnetic field deviation of the ST and DT4 dipoles at 1715 A/s and 1200 A. The magnetic field deviation is defined as the difference between the measured AC magnetic field and the DC magnetic field at the same current [13]. The magnetic field deviations of the ST and DT4 dipoles are 0.35 and 0.29%, respectively. The delays of eight mass-produced dipoles with ST endplates are almost identical.

The delay time and magnetic field deviation at different maximum currents are shown in Fig. 3. The delay time is defined as the time from the end of ramping to the instant when the magnetic field deviation becomes less than 0.02%. The maximum delay time is approximately 1 s. This means that extraction should start after a long wait after ramping up. The measurement results also show that the delay time and magnetic field deviation increase with the ramping rate. The time constant for different ramping rates and maximum currents is approximately 0.24 s; this value decreases slightly along the ramp. In fact, it is much smaller than the theoretical value obtained from Eq. (1). This shows that the iron permeability becomes smaller owing to saturation. The magnetic field deviation and time delay increase with the maximum current, but reach their maximum at a current of approximately 1000 A.

The fields at different points along the central line are measured to understand the effect of the eddy current at different longitudinal positions. Figure 4 shows the magnetic field of DT4 and ST dipoles at different points. The measurement results agree with the theory. The ramping of magnetic field leads to variation in the strength of eddy current with the longitudinal position. Because the eddy current diffuses along the magnet, the vertical field component decreases the main field at the yoke end and

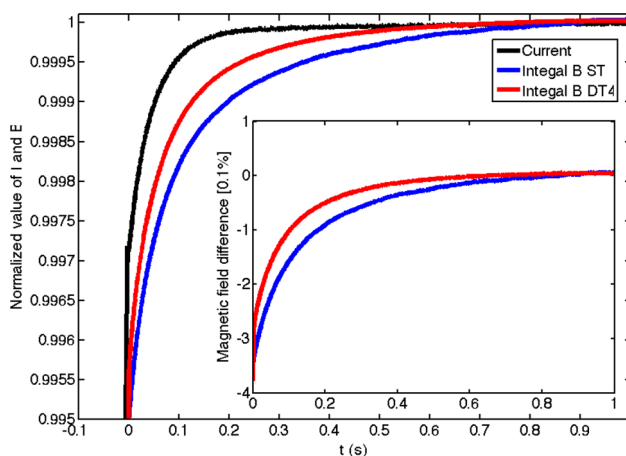


Fig. 2 (Color online) Normalized current, integral magnetic field, and magnetic field deviation

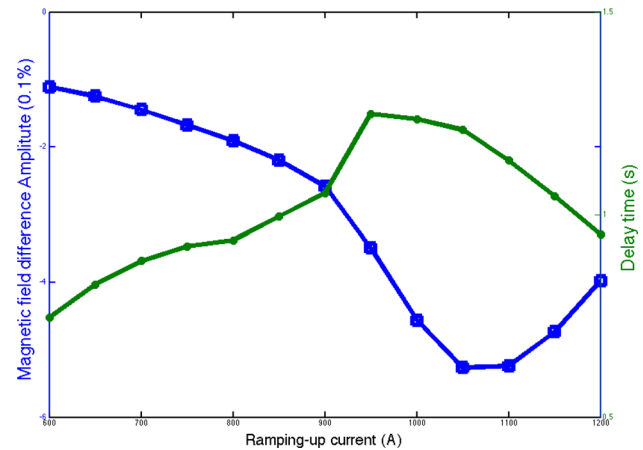


Fig. 3 (Color online) Delay time and magnetic field deviation with current

increases the main field at the center of the magnet [11]. The magnetic field delay at 1200 A is smaller than that at 1000 A at the edge of the magnet. The magnetic field deviation of DT4 dipole is also smaller than that of ST dipole. All these measurements agree with the AC magnetic field measurements.

4 Three-dimensional time-dependent simulations

In order to understand the eddy current and find optimizations to reduce the effect, several simulations are performed under conditions identical to the measurement conditions. The OPERA-3D/ELEKTRA transient module is used for the simulation. Figure 5 shows the eddy current density in the dipoles with different endplate materials at the same time (0.4 s), same ramping rate (1715 A/s), and same maximum current (1200 A). The measured current curve of the power supply is used in the simulation. Eddy currents in the laminate of the two types of dipoles are almost identical. The eddy current in the endplates of the ST dipole is much smaller than that in the DT4 dipole. The simulation shows some very high saturation points.

In the endplate, the large eddy current is located under the bedstead coil. The bedstead coil makes the magnet compact, both vertically and longitudinally. However, the coil creates field components perpendicular to the laminations B_z , which induce eddy currents within the laminations. Simulation shows that the racetrack coil does not create such components. The eddy current will decrease by a factor of 2. The measured eddy current in the racetrack-coil-type dipole is also quite small [9].

Figure 6 shows the integral magnetic field and the magnet field at different points of the ST dipole. The magnetic deviations of the ST and DT4 dipoles are 0.4 and 0.6%, respectively, at 1715 A/s and 1200 A. The eddy

Fig. 4 (Color online) Magnetic field error at different points. Figures at the top are for DT4 dipoles, and those at the bottom are for ST dipoles

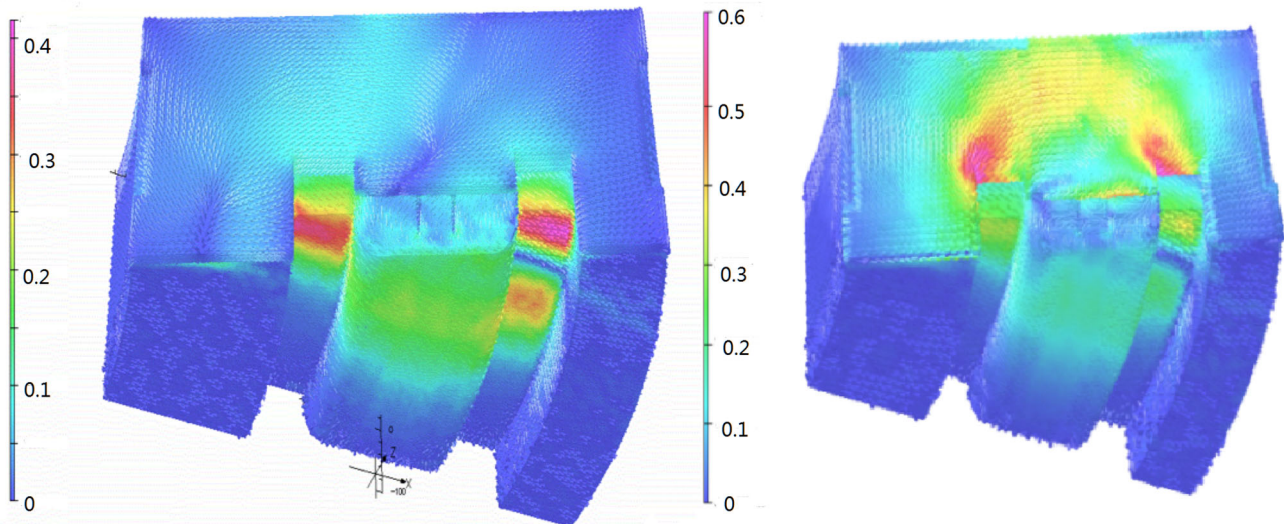
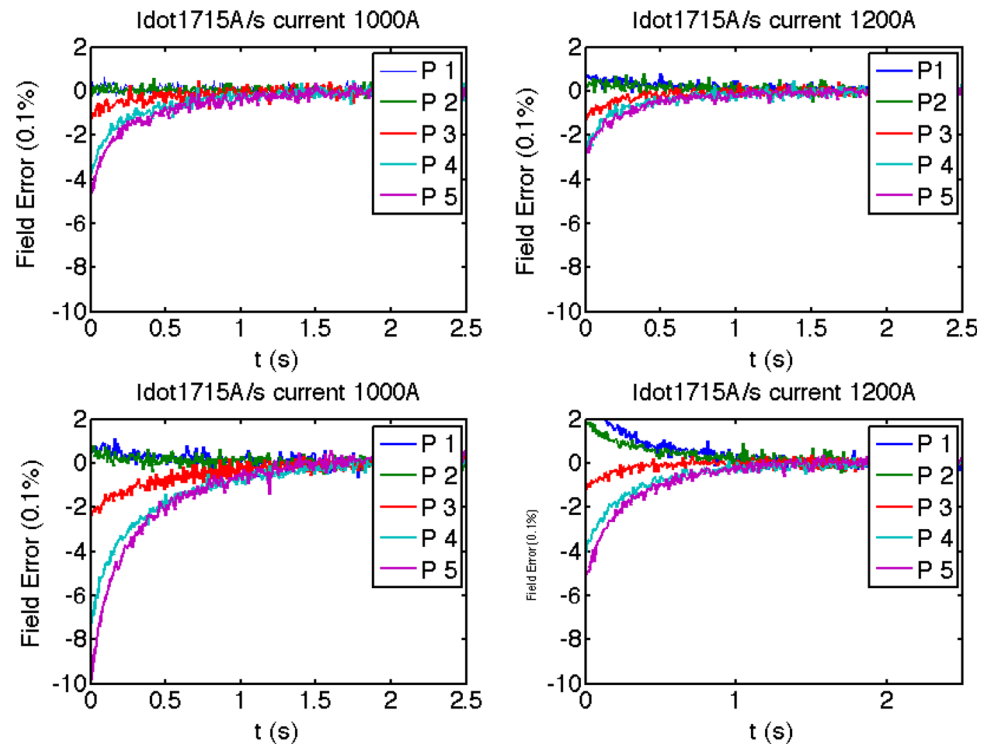


Fig. 5 (Color online) Eddy current density under identical conditions. The endplates of the left dipole are made of stainless steel, while those of the one on the right are made of DT4

current increases with magnet field strength, but reaches a maximum at 1000 A. The ANSYS simulation also yields the same results. The simulations of the ST dipole agree well with the measurements. However, the simulations of the DT4 dipole do not agree with the measurement results, and more study is required into this. The pure iron endplate contributes only partially to the integral field, as it does not cover the pole completely. However, the pure iron endplate results in a complicated flux pattern at the ends, with high

saturation points. Owing to its low resistance, the eddy currents increase.

In the simulations and prototype, the dipole is one block (the laminates are stacked in parallel and cut at 22.5° at the ends). This packing method leads to lower μ at the end, and the laminates at the end are short-circuited. Both these factors lead to an increase in eddy currents. A five-block-type dipole is also simulated. Figure 7 shows the integral

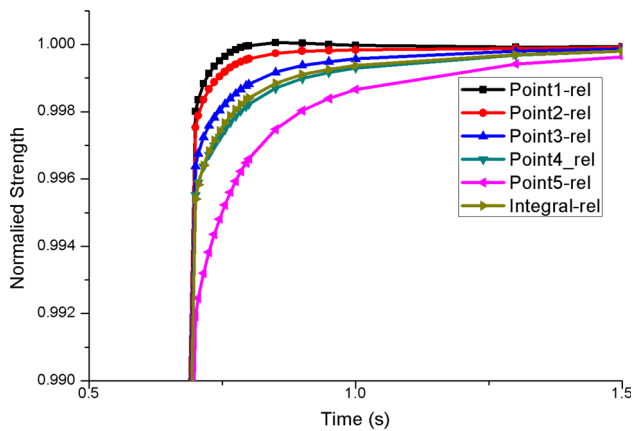


Fig. 6 (Color online) Integral magnet field and magnet field of the ST dipole

magnetic field deviation for one block and five blocks; the value decreases to 0.3%.

5 Compensation using a power supply

Measurements and simulations show that a time delay is always present. It can only be partially reduced. In order to reduce the waiting time caused by the eddy current, field control using a power supply is employed. Two ways to achieve this are via feedback and feedforward. In the so-called real-time field control feedback scheme, the difference between the measured field and the set value is added to the current control loop of the power supply of the magnet [16]. The difference is obtained by the pickup coil [11] or beam tracking code [17]. In the feedforward scheme, the magnetic field and current of the power supply are measured and optimized offline. In the case of a resonant power supply, harmonics are injected to reduce the

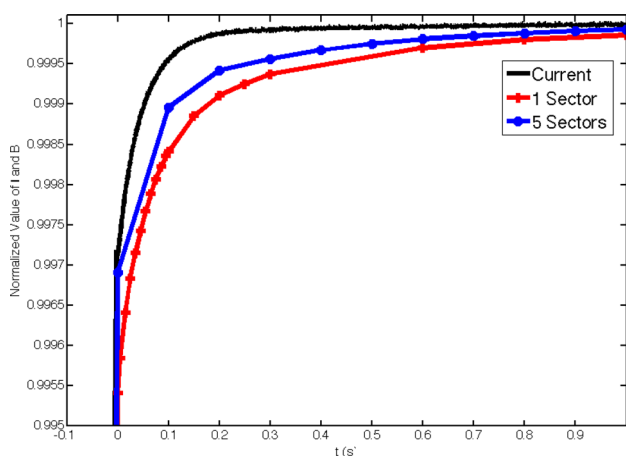


Fig. 7 (Color online) Integral magnet field for one block and five blocks

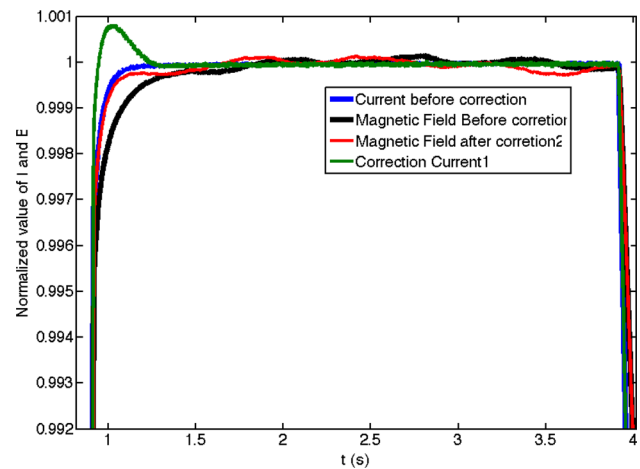


Fig. 8 (Color online) Magnet field and current after correction

magnetic tracking errors [18]. In the case of a digital power supply, a linear excitation current overshoot at the end of ramp-up can partially or totally cancel the time delay [17]. Figure 8 shows the overshoot and the correction results. After correction, the magnetic field deviation decreases to less than 0.02%. The waiting time or orbit correction that is required because of the eddy current is no longer needed.

6 Conclusion

Eddy current introduces a time delay and thus affects the beam. Simulations and measurements show that the maximum magnetic field deviation of the ST dipole at 1200 A is approximately 0.4%. The main sources of eddy current are the field components B_z introduced by the bedstead coil and saturation. The racetrack coil and five-block design will reduce the eddy current. Field correction by overshoot at the end of ramp-up reduces the magnetic field deviation to less than 0.02%. The simulations do not agree with the measurements for the DT4 dipole, and more research is required into this.

Acknowledgements The authors would like to thank the entire SAPT team for their innovation and commitment. Dr. Moritz, Dr. Wen Kang, and Dr. Qiao-Gen Zhou gave us numerous suggestions for the design and simulation.

References

1. D. Shi, L.H. Ouyang, M. Gu, The RF-knockout slow-extraction for Shanghai proton therapy facility. *Nucl. Tech.* **35**, 231–235 (2012). (in Chinese)
2. Y.H. Yang, M.Z. Zhang, D.M. Li, Simulation study of slow extraction for the Shanghai advance proton therapy. *Nucl. Sci. Tech.* **28**, 120 (2017). <https://doi.org/10.1007/s41365-017-0273-0>

3. U. Amaldi, M. Grandolfo, L. Picardi, The TERA project and the design of compact proton accelerators (The TERA Collaboration, 1995)
4. M.G. Pullia, Synchrotrons for Hadrontherapy, in *Reviews of accelerator science and technology*, vol. 2, ed. by A.W. Chao (World Scientific Publishing Company, Singapore, 2009), pp. 157–178
5. Z.X. Yang, M.Z. Zhang, D.M. Li, Optimization of ripple filter for pencil beam scanning. *Nucl. Sci. Tech.* **24**, 060404 (2013). <https://doi.org/10.13538/j.1001-8042/nst.2013.06.021>
6. P.J. Bryant, L. Badano, M. Benedikt, et. al., Proton-ion medical machine study (PIMMS), CERN 9-134 (1999). <https://doi.org/10.1007/bf03038873>
7. B. Langenbeck, C. Siedler, M. Stockner, et.al. Design and optimization of the MedAustron synchrotron main dipoles, in *Proceedings of IPAC2011* (San Sebastián, Spain, 2011) pp. 2406–2408
8. R. Chritin, Recent advances in pulsed-mode measurements at CERN, in *International Magnet Measurement Workshop* (IMMW18), Brookhaven (2013)
9. G. Moritz, *Eddy currents in accelerator magnets* (CERN Accelerator School-Magnets, Bruges, 2009)
10. A. Peters, E. Feldmeier, C. Schömers et.al., Magnetic field control in synchrotrons, in *Proceedings of PAC09*, Vancouver, BC, Canada (2009), pp. 169–171
11. R. Chritin, Measuring eddy current contributions in normal conducting magnets, in *IMMW17*, La Mola, Spain, 2012
12. G. Golluccio, Overview of the magnetic measurements status for the MedAustron project, in *IMMW18*, Brookhaven (2013)
13. J.X. Zhou, DC&AC magnetic field measurement of the CSNS/RCS quadrupole magnet, in *IMMW18*, Brookhaven (2013)
14. C.D. Deng, F.S. Chen, X.J. Sun et al., Develop of CSNS magnet system and prototype. *Chin. Phys. C* **S1**, 71–73 (2008). (in Chinese)
15. S.I. Kukarnikov, V.K. Makoveev, A. Yu. Molodozhentsev, et.al. Design of the dipole and quadrupole magnets of the PRAMES, in *Proceeding of EPAC98*, Stockholm City, Sweden, 1998, pp. 1213–1215
16. E. Feldmeier, T. Haberer, M. Galonska et.al. The first magnetic field control (B-Train) to optimize the duty cycle of a synchrotron in clinical operation, in *Proceedings of IPAC2012*, New Orleans, Louisiana, USA, THPPD002 (2012), pp. 3503–3505
17. A. Beaumont, M. Buzio, D. Giloteaux, et.al., Real-time magnetic field control applications at CERN: an update, in *IMMW18*, Brookhaven (2013)
18. S.Y. Xu, The harmonic injection for resonant power supply system of CSNS/RCS, ICFA Mini-Workshop on Beam Commissioning for High Intensity Accelerators, Dongguan, Guangdong, P.R. China, 2015